Effect of low-temperature baking on the radio-frequency properties of niobium superconducting cavities for particle accelerators

Gianluigi Ciovati[a)]
Thomas Jefferson National Accelerator Facility, Newport News, Virginia 23606
and Department of Physics, Old Dominion University, Norfolk, Virginia 23529

(Received 19 March 2004; accepted 7 May 2004)

Radio-frequency superconducting (SRF) cavities are widely used to accelerate a charged particle beam in particle accelerators. The performance of SRF cavities made of bulk niobium has significantly improved over the last ten years and is approaching the theoretical limit for niobium. Nevertheless, RF tests of niobium cavities are still showing some "anomalous" losses that require a better understanding in order to reliably obtain better performance. These losses are characterized by a marked dependence of the surface resistance on the surface electromagnetic field and can be detected by measuring the quality factor of the resonator as a function of the peak surface field. A low-temperature (100–150 °C) "*in situ*" bake under ultrahigh vacuum has been successfully applied as final preparation of niobium RF cavities by several laboratories over the last few years. The benefits reported consist mainly of an improvement of the cavity quality factor at low field and a recovery from "anomalous" losses (so-called "*Q* drop") without field emission at higher field. A series of experiments with a CEBAF single-cell cavity have been carried out at Jefferson Lab to carefully investigate the effect of baking at progressively higher temperatures for a fixed time on all the relevant material parameters. Measurements of the cavity quality factor in the temperature range 1.37–280 K and resonant frequency shift between 6–9.3 K provide information about the surface resistance, energy gap, penetration depth, and mean free path. The experimental data have been analyzed with the complete BCS theory of superconductivity. The hydrogen content of small niobium samples inserted in the cavity during its surface preparation was analyzed with nuclear reaction analysis. The single-cell cavity has been tested at three different temperatures before and after baking to gain some insight on thermal conductivity and Kapitza resistance and the data are compared with different models. This paper describes the results of these experiments and comments on existing models to explain the effect of baking on the performance of niobium RF cavities. © *2004 American Institute of Physics*. [DOI: 10.1063/1.1767295]

I. INTRODUCTION

The performance of a superconducting cavity for particle accelerators is characterized by a plot of the quality factor Q_0 as a function of the accelerating field E_{acc} (excitation curve) for the mode TM_{010}. The quality factor $Q_0=\omega U/P$ is defined as the ratio between the cavity stored energy and the power dissipated in the cavity walls in one RF radian. It can also be defined as $Q_0=G/R_s$, where G is the geometrical factor (in Ω) of the cavity and is a function only of the cavity shape (not of its size or material), and R_s is the RF surface impedance of the cavity material. Thus R_s can be obtained directly from a measurement of Q_0. The accelerating field is defined as the ratio of the accelerating voltage V_{acc} (energy gained by a particle's going through the cavity and the particle's charge) and the cavity length.

The excitation curve of a superconducting cavity, made of bulk niobium, in the GHz range shows three distinct regions where the quality factor Q_0 changes with the accelerating gradient E_{acc}. An increase of Q_0 is often seen at E_{acc} below 4 MV/m. It is usually followed by slow Q_0 degradation, up to 20–30 MV/m, when Q_0 starts to decrease more rapidly, even in the absence of field emission (Fig. 1). Baking the cavities between 100 °C and 150 °C under ultrahigh vacuum for more than 24 h has been seen to have beneficial effects on the BCS surface resistance and the high-field *Q* drop. It has been related to oxygen diffusion into the niobium,[1,2] causing changes of the structure of the niobium/oxide interface on a nanometer scale.

In this work we study carefully and systematically the effects of baking on the Q_0 versus field nonlinearity and on the superconducting parameters.

While the effect of baking on the oxide layer has been extensively studied in several laboratories, a lot less is known about the effect of hydrogen, whose presence in niobium has been shown to be problematic.[3] To gain some understanding in this direction, the hydrogen distribution in niobium samples baked with the cavity has been analyzed

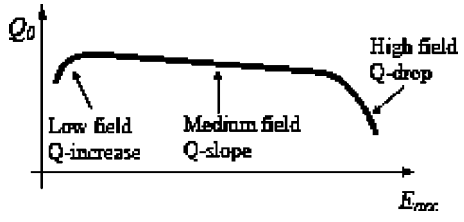

FIG. 1. *Q* vs field "anomalous" behaviors.

[a)]Electronic mail: gciovati@jlab.org

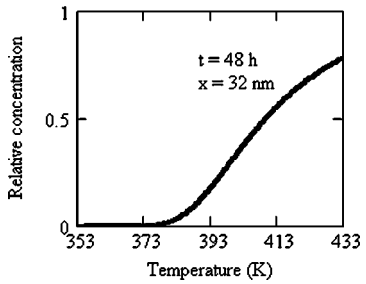

FIG. 2. Oxygen concentration relative to the surface as a function of temperature in kelvin at a depth of 32 nm.

with nuclear reaction analysis NRA (Ref. 4) at SUNY Albany and compared with samples that have not been baked.

II. EXPERIMENTAL SETUP AND PROCEDURES

RF tests have been conducted on a single-cell cavity in the TM_{010} mode at 1.467 GHz. The geometry of the cavity is the same as the one used in the CEBAF accelerator.[5] The main electromagnetic parameters of RF cavity are the ratio between peak surface electric field and accelerating field E_{peak}/E_{acc}, where the accelerating field is calculated as the ratio between the accelerating voltage for a particle going through the single-cell cavity and the cavity length; the ratio between peak surface magnetic field and accelerating field B_{peak}/E_{acc}; the ratio of the shunt impedance R divided by the quality factor, $R/Q_0=V_{acc}^2/\omega U$, which is the ratio between the accelerating voltage squared and the energy stored in one radian (depends only on the cavity shape and is an indication of the efficiency of the acceleration); and the geometry factor G. The CEBAF single-cell cavity has the following values of the electromagnetic parameters: $E_{peak}/E_{acc}=1.78$, $B_{peak}/E_{acc}=4.43$ mT/(MV/m), $R/Q_0=96.5\ \Omega$, $G=273\ \Omega$. Prior to stamping the half cells, the niobium disks were postpurified in a titanium box at 1400 °C for 4 h. After electron-beam welding half cells and beam tubes, the cavity had a prechemistry with buffered chemical polishing (BCP).

The preparation for the tests involves the following steps.

(1) Ultrasonic degreasing for 20 min.
(2) BCP with HNO_3, HF, H_3PO_4(1:1:1) for 1 min, removing about 7 μm.
(3) High-pressure rinsing between 40 min and 1.5 h with ultra pure water at a pressure of 80 bar and a flow rate of 15 l/min.

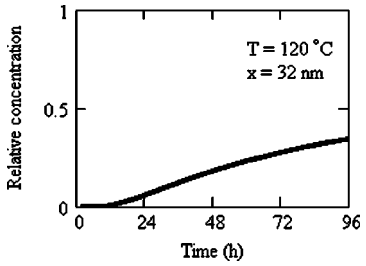

FIG. 3. Oxygen concentration relative to the surface as a function of time in hours at a depth of 32 nm and at a temperature of 120 °C.

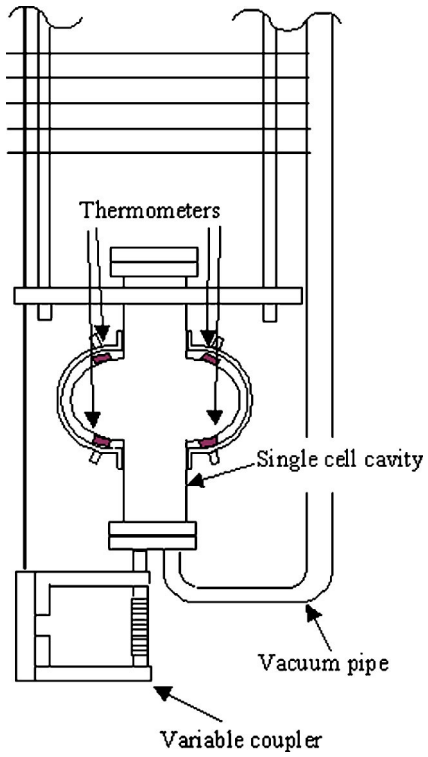

FIG. 4. Schematic of the experimental setup.

(4) Assembly of a variable input coupler, providing Q_{ext} adjustable between 10^7 and 10^{11}, and of a fixed transmission probe. The assembly is done in a class 10 clean room.
(5) The cavity is attached to a vertical test stand and evacuated to about 10^{-8} mbar using a turbo-molecular pump backed by a scroll pump.
(6) Four calibrated Cernox® thermometers (two at the top iris, two at the bottom iris) are pushed against the cavity with the aid of an aluminum frame; Apiezon® grease between thermometers and cavity is used to ensure a good thermal contact.

Two niobium samples are prepared with the cavity and one of them is inserted into the pumping line of the test stand.

After cool down in a dewar filled with liquid helium to 4.2 K the following tests are performed.

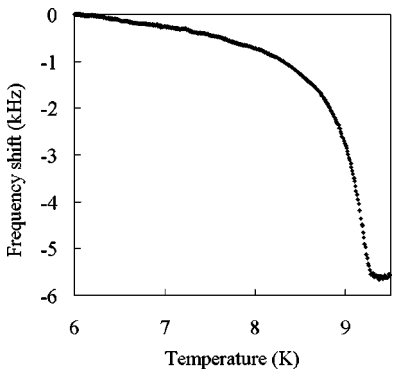

FIG. 5. Typical frequency shift vs temperature close to T_c at 1.467 GHz. Data are acquired every 30 s.

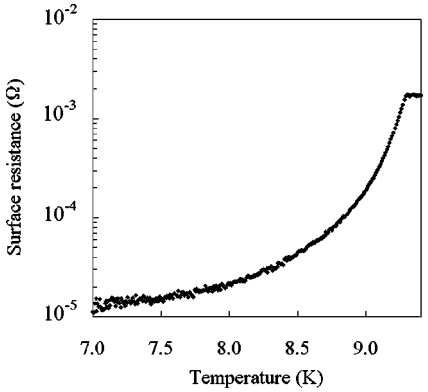

FIG. 6. Typical surface resistance vs temperature close to T_c at 1.467 GHz.

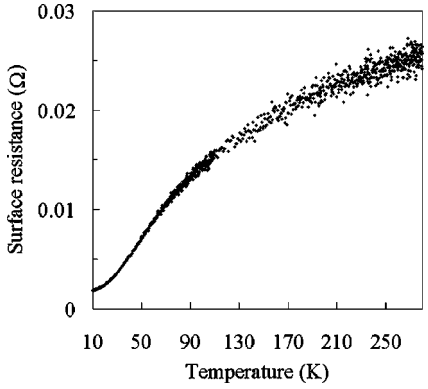

FIG. 7. Typical surface resistance vs temperature in the normal conducting state.

(1) Q_0 versus temperature is measured between 4.2 K and 1.37 K at a peak magnetic field of 4 mT. The temperature is obtained from the helium pressure measured with a calibrated Baratron® gauge.
(2) Q_0 vs. E_{acc} is measured at 2.2, 2, and 1.37 K.
(3) Liquid helium is boiled off with a heater and then the cavity is warmed up through the dewar static heat leak. Frequency and Q_0 are measured with a network analyzer in the temperature range 6–280 K, obtained as the average of the four Cernox readings. The network analyzer excites the cavity at very low field levels ($E_{peak} \approx 0.8$ MV/m). The data are automatically acquired with a Labview® program.
(4) The test stand with the cavity and the sample are baked *in situ* at a fixed temperature for 48 h plus 2 h for temperature ramp-up and ramp-down. Two heaters blowing hot nitrogen in an oven are used to raise the temperature that is controlled within 1 °C. The partial pressures of the main gas species are recorded with a residual gas analyzer during bake-out. The cavity is kept under vacuum during bake-out.
(5) The measurements listed in the first three points are repeated on the baked cavity.
(6) The cavity is finally disassembled and processed again for baseline tests and baking at another temperature.

The warm up between 4.2 K and 9.5 K takes about 9 h and the temperature difference across the cavity is less than 15 mK. The dewar is also opened to atmosphere so that the pressure is constant within 2 mbar. These procedures assure a very accurate measurement of frequency, Q_0, and temperature.

We choose to bake the cavity for a fixed amount of time because, according to the solution of the diffusion equation,[1] it is faster to change the concentration of oxygen at a depth of the order of the RF penetration depth by increasing the baking temperature than by increasing time, as can be seen in Figs. 2 and 3. Figure 4 shows a sketch of the experimental setup.

III. TEST RESULTS

The values of the surface resistance are obtained from Q_0 through the relation $R_s = G/Q_0$ while the variation of the

TABLE I. Material parameters before and after baking at different temperatures which are obtained below 4.2 K at 40 nm depth from the surface and between 7 K and 9.1 K for 300 nm.

	Δ/kT_c (40 nm)	l (40 nm) (nm)	l (300 nm) (nm)	λ (0 K) (nm)	Surf. RRR
Baseline	1.89±0.03	364±187	954±38	46±1	255±26
50 °C bake	1.84±0.03	193±76	785±36	46±1	255±26
Baseline	1.81±0.01	695±187	990±61	47±1	195±20
70 °C bake	1.84±0.02	483±130	671±72	43±1	220±22
Baseline	1.85±0.02	1455±611	697±27	45±1	189±19
90 °C bake	1.85±0.02	178±60	514±13	40±1	191±19
Baseline	1.79±0.03	387±190	1077±47	44±1	175±18
105 °C bake	1.82±0.02	64±31	708±14	42±1	209±21
Baseline	1.80±0.02	476±150	854±38	36±1	216±22
120 °C bake	1.89±0.01	26±118	354±78	36±1	211±21
Baseline	1.78±0.02	250±71	1024±42	38±1	218±22
140 °C bake	1.89±0.01	27±102	454±67	32±1	181±18
Baseline	1.81±0.02	508±157	784±90	41±1	196±20
160 °C bake	1.85±0.01	27±74	12±1	78±1	136±14
Baseline	1.85±0.02	841±338	994±81	42±1	196±20
180 °C bake	1.85±0.02	18±16	130±1	92±4	97±10

TABLE II. BCS surface resistance at T=4.2 K, B_{peak}=4 mT, residual resistance and high-field (B_{peak}>75 mT) limitations.

	R_{BCS} (4 K) ($n\Omega$)	R_{res} (nΩ)	Limitation
Baseline	844±59	4.9±0.6	FE β=230
50 °C bake	816±57	2.4±0.3	FE β=179
Baseline	1130±79	4.4±0.2	Quench
70 °C bake	1048±73	6.4±0.3	Quench
Baseline	1148±80	5.2±0.2	FE β=185
90 °C bake	849±59	5.9±0.2	FE β=177
Baseline	1112±78	7.4±0.3	FE β=165
105 °C bake	717±50	10.3±0.3	FE β=280
Baseline	1110±78	6.9±0.2	Q-drop
120 °C bake	542±38	6.4±0.1	Quench
Baseline	1059±74	5.4±0.2	FE β=192
140 °C bake	565±40	8.9±0.2	FE β=188
Baseline	1110±78	4.0±0.2	Q drop
160 °C bake	618±43	7.5±0.2	Quench
Baseline	1090±76	4.2±0.2	Q drop
180 °C bake	610±43	8.0±0.2	Quench

penetration depth λ is obtained from the resonant frequency shift $[f(T)-f(T_0)]$ between 6 K and 9.3 K according to the following formula:[6]

$$\lambda(T)-\lambda(T_0)=\frac{G}{\mu_0\pi f^2(T_0)}[f(T)-f(T_0)], \quad (1)$$

where T_0 is typically 6 K. Furthermore, the surface resistance is expressed as the sum of the BCS term and a residual term R_{res}. The residual resistance is temperature independent and is related to many causes: surface imperfections and inclusions, residual dc magnetic field (which for our test setup is about 3×10^{-4} mT), condensed gases, etc.

The surface resistance and the penetration depth data are fitted with a computer code[7] that includes the complete BCS theory calculation for diffuse electrons at the surface, as written by Halbritter.[8] The parameters obtained from the fits are the critical temperature (T_c), the energy gap at 0 K[$\Delta(0)$], the mean free path of the normal electrons (l), the residual resistance (R_{res}), and the penetration depth at 0 K[$\lambda(0)$]. It has been shown that these parameters are strongly dependent on the surface condition,[9,10] while the values of the London penetration depth λ_L and the coherence length $\xi_F=\pi\xi_{BCS}/2$ are considered material constants equal to 32 nm and 62 nm, respectively.[11]

The surface resistance in the normal conducting state has been fitted with a computer code[12] that includes the anomalous skin effect and the values of the surface resistivity $[\rho(T)]$ at 10 K and 300 K are obtained. The ratio $\rho(300\text{ K})/\rho(10\text{ K})$ defines the residual resistivity ratio (RRR) which is related to the impurity content in the material.

The fit of the surface resistance data between 4.2 K and 1.37 K yields the material parameters in the RF penetration depth that is about 40 nm at those temperatures. Close to T_c, RF fields penetrate about 300 nm into the surface, and material parameters obtained from the fit of surface resistance and penetration depth with the BCS theory are relative to such depth.

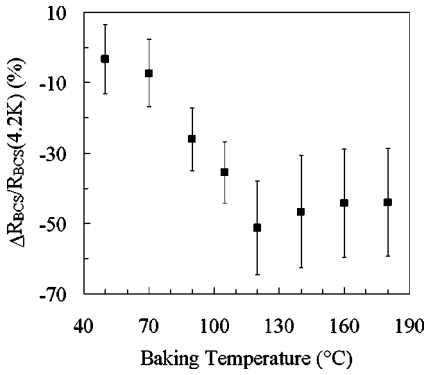

FIG. 8. Variation of BCS surface resistance at 4.2 K as a function of baking temperature.

Figures 5 and 6 show examples of the typical frequency shift and surface resistance versus temperature above 6 K. Figure 7 shows the typical surface resistance in the normal conducting state versus temperature.

The results from the data fits are shown in Table I. The value of mean free path over a 300 nm depth and of T_c are the weighted average of the values obtained from the surface resistance and penetration depth fit between 7 K and 9.1 K. The average value of the RRR before baking is 205±3 which corresponds to an oxygen concentration of 0.017 at. %.[13] The bulk RRR after postpurification heat treatment is estimated to be greater than 300.

The values of BCS surface resistance at 4.2 K and of the residual resistance, measured at B_{peak}=4 mT, are indicated in Table II, along with the performance limitation at high field (E_{peak}=32−53 MV/m, B_{peak}=80−133 mT). FE refers to field emission and β is the field enhancement factor.

Table II and Fig. 8 show that BCS surface resistance decreases by as much as 50% after baking and this effect is related to a reduction in the mean free path, summarized in Fig. 9. Since surface resistance has a weak dependence on mean free path, the values obtained from the fits in the 4.2–1.37 K range have large errors. The penetration depth has a stronger dependence on mean free path and therefore l is obtained more accurately from the measurements between 7 K and 9.1 K. Even though the value of the mean free path after a new chemical etching can change by as much as 40% (between 700 nm and 1200 nm), the relative variation before and after baking is well correlated with the baking temperature.

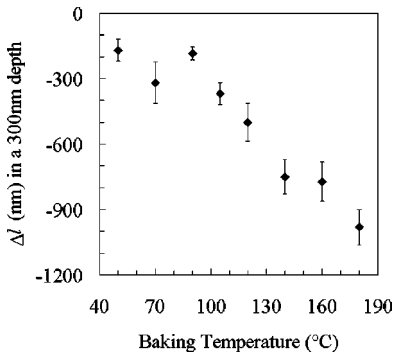

FIG. 9. Variation of mean free path as a function of the baking temperature.

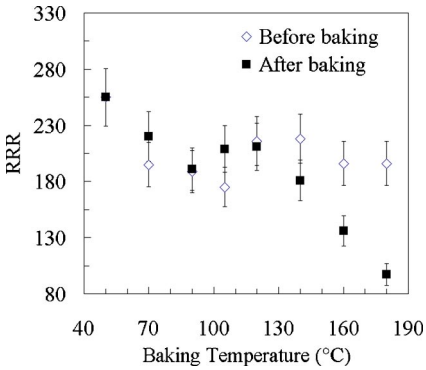

FIG. 10. Surface RRR as a function of baking temperature.

The dependence of residual resistance on baking temperature does not show a clear trend, although baking generally increases it. The values of residual resistance in the baseline tests differ by as much as a factor of 2, between 4 nΩ and 7.4 nΩ and the cause for such variations can be assumed to be related to different Nb-Nb_2O_5 morphology.

The average value of $\Delta(0\ \mathrm{K})/kT_c$ in the 40 nm depth before baking is 1.823 ± 0.006 and after baking is 1.853 ± 0.008, consistent with values obtained for oxidized niobium.[8] The surface RRR clearly starts to decrease for baking temperatures higher than 120 °C and this effect is consistent with the model of deeper oxygen diffusion in niobium at progressively higher temperatures (Fig. 10).

The average value of the critical temperature before baking is 9.252 ± 0.004 K and it is 9.241 ± 0.005 K after baking. This decrease can also be explained by oxygen diffusion in the material.[11]

Figure 11 shows the partial pressure of the three main gas species after baking for 24 h as a function of the baking temperature. The exponential increase in the hydrogen partial pressure can be noticed.

The results from the NRA measurements on samples are shown in Fig. 12: the hydrogen concentration is significantly reduced in the baked samples. The depth resolution of this measurement is about 5 nm.

High-power RF tests reveal the high-field Q drop without field emission on two occasions. The first time the cavity was baked at 120 °C for 48 h, after which the Q drop became negligible and the cavity quenched at a peak magnetic

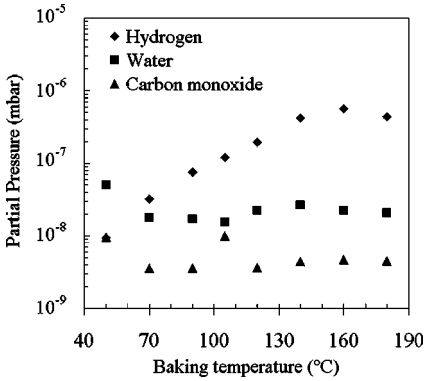

FIG. 11. Partial pressure for the three main gases registered after baking for 24 h vs baking temperature.

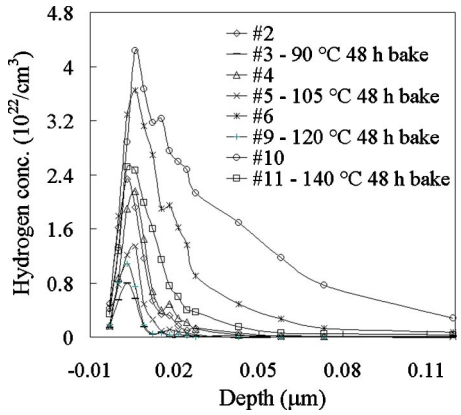

FIG. 12. Hydrogen concentration vs depth for samples baked and not baked.

field of 130 mT (Fig. 13). In this case the residual resistance after baking did not increase and there was also an enhancement of the low-field Q slope.

Figures 14–16 show for both cases the temperature dependence of the surface resistance below 4.2 K, close to T_c, and the variation of penetration depth, respectively.

In the second case, the cavity was baked at 160 °C for 48 h following which (Fig. 17) the Q drop became negligible and the cavity quenched at 114 mT peak magnetic field. In this case the residual resistance increased by baking and there is an enhancement of the low-field Q slope. The large variation in the mean free path after baking can be easily detected through the penetration depth, as shown in Fig. 18.

In a third case, the characteristic behavior of the Q drop was observed but in the presence of some field emission. The cavity was baked at 180 °C for 48 h, after which it quenched at 110 mT peak magnetic field (Fig. 19).

IV. MODELS COMPARISONS

Surface analysis studies[2,14–16] on niobium samples indicate that baking at progressively higher temperatures causes a conversion of the external Nb_2O_5 layer to metallic suboxides (NbO, NbO_2) and an overall reduction of the oxide layer thickness. The RF measurements reported here are consistent with those results: above about 100 °C the surface RRR and mean free path are decreased, due to oxygen injection into

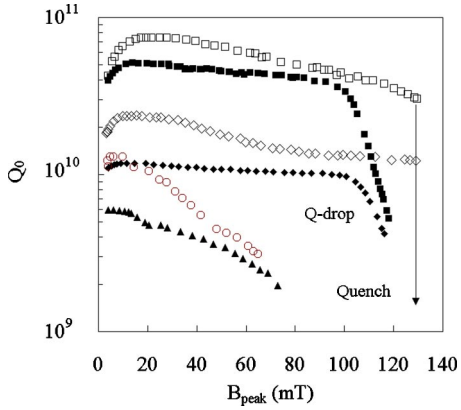

FIG. 13. Q_0 vs B_{peak} before (solid symbols) and after 120 °C, 48 h baking (open symbols) at three different temperatures: 1.37 K (squares), 2 K (diamonds), and 2.2 K (triangles).

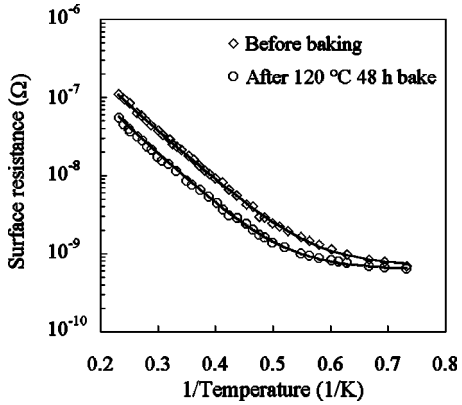

FIG. 14. Surface resistance vs 1/temperature before and after 120 °C, 48 h baking. The solid lines represent the results from the fit using the BCS surface resistance plus the residual term.

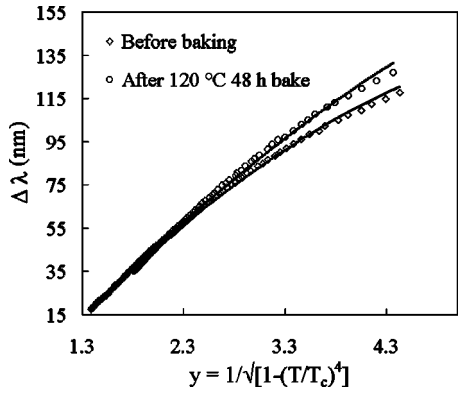

FIG. 16. Variation of penetration depth as a function of the reduced temperature parameter y before and after 120 °C, 48 h baking. The solid lines represent the results from the fit using the BCS theory.

the niobium, causing a reduction of the BCS surface resistance, as predicted by the BCS theory. Another indication that oxygen is the impurity involved in the baking process is an early measurement of oxygen concentration versus depth, extracted from the variation of the BCS surface resistance,[17] which was very well described quantitatively by the oxygen diffusion profile for that particular combination of baking time and temperature.[1] The facts that hydrogen is mobile in niobium at room temperature and that NRA measurements show its concentration to be decreased after baking are not consistent with the observed material parameters variations.

According to this modeling of the baking effect, a cavity that would be baked at progressively higher temperature, instead of being chemically etched to form a new oxide layer before each baking, should show a continuous decrease of the BCS surface resistance due to oxygen diffusion up to a "saturation" point when the oxide layer had been significantly depleted. This view is supported by measurements done by Kneisel[17] on a cavity baked at 140 °C for progressively longer times.

A. Low-field *Q* slope

According to Halbritter's model for the decrease of surface resistance at low field,[18] this "anomalous" behavior is due to the presence of niobium suboxides that introduce quasiparticle states inside the energy gap. These states are locally confined and occupied at low field and temperature, yielding a mean value of energy gap Δ^* lower than the one corresponding to pure niobium. The surface resistance $[\propto \exp(-\Delta^*/kT_c)]$ is therefore higher at low field. With increasing RF field, the confined quasiparticles are driven out from those suboxide states above the energy gap, restoring the proper value of energy gap. This effect saturates above about $B_{\text{peak}} = 12$ mT. Baking forms additional NbO_x clusters in the niobium and the low-field Q slope is enhanced. According to this model, surface resistance is predicted to be inversely proportional to the square of the peak magnetic field. We fitted the surface resistance at low field according to the following formula:

$$R_s = a/B_{\text{peak}}^2 + b, \tag{2}$$

which describes quite well the data before and after baking (Fig. 20). The average correlation factor r^2 over 24 fits is 0.938. The average values of the fitting parameters a and b at 2 K and 1.37 K, before and after baking are indicated in Table III. The low-field Q slope can be present also before baking, depending on the amount of NbO_x clusters and therefore on the oxidation condition.

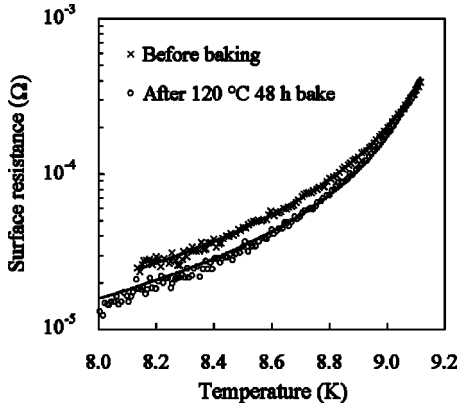

FIG. 15. Surface resistance vs temperature close to T_c before and after 120 °C, 48 h baking. The solid lines represent the results from the fit using the BCS surface resistance plus the residual term.

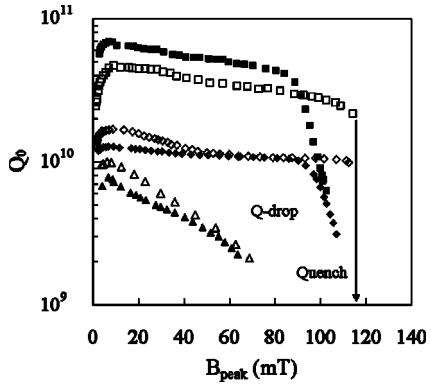

FIG. 17. Q_0 vs B_{peak}before (solid symbols) and after 160 °C, 48 h baking (open symbols) at three different temperatures: 1.37 K (squares), 2 K (diamonds), and 2.2 K (triangles).

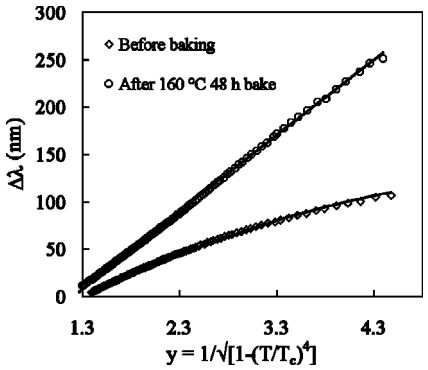

FIG. 18. Variation of penetration depth as a function of the reduced temperature parameter y before and after 160 °C, 48 h baking. The solid lines represent the results from the fit using the BCS theory.

B. Medium field *Q* slope

Above about 12 mT peak magnetic field, the cavity quality factor decreases with increasing field, causing a medium field Q slope that is temperature dependent. All the models that try to explain this effect involve heating of the inner surface of the cavity with respect to the helium bath due to low thermal conductivity and Kapitza resistance of niobium. The data have been analyzed according to three models.

(1) Halbritter proposed the following Taylor series of the surface resistance, obtained from the Ginzburg-Landau theory:[19]

$$R_s = R_{s0}[1 + \gamma(B_{\text{peak}}/B_c)^2 + O(B_{\text{peak}}^4)], \tag{3}$$

where $R_{s0}(=R_{\text{res}}+R_{\text{BCS}})$ and γ are fitting parameters. The following expression was obtained for γ, which represents the slope:

$$\gamma = R_{\text{BCS}}(T_0)B_c^2\Delta/(2kT_0^2)(d/\kappa + R_k), \tag{4}$$

where κ is the thermal conductivity, R_k is the Kapitza resistance, d is the wall thickness, T_0 is the helium bath temperature, and B_c is the critical field $B_c(0) \cong 200$ mT. Figure 21 shows an example of the data and fit according to this model.

(2) The data are usually well described empirically by a linear dependence of the surface resistance from the peak magnetic field:

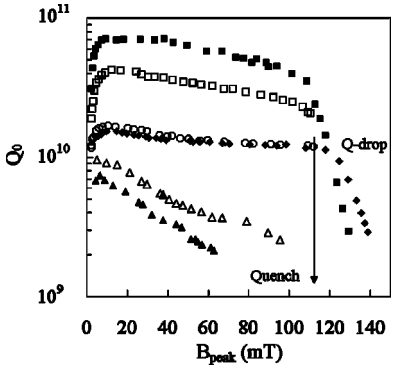

FIG. 19. Q_0 vs B_{peak} before (solid symbols) and after 180 °C, 48 h baking (open symbols) at three different temperatures: 1.37 K (squares), 2 K (diamonds), and 2.2 K (triangles).

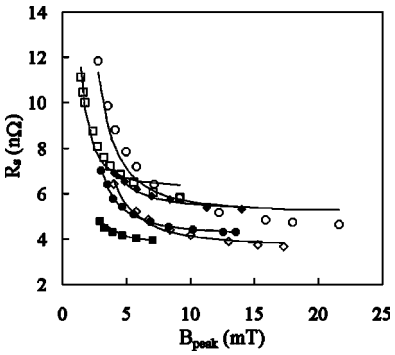

FIG. 20. Surface resistance vs B_{peak} at low field and 1.37 K; data are fitted to function (2) before (solid symbols) and after baking (open symbols) at three different temperatures: 120 °C (triangles), 140 °C (circles), and 160 °C (squares).

$$R_s = a + bB_{\text{peak}} + O(B_{\text{peak}}^2), \tag{5}$$

where a and b are fitting parameters.

(3) Visentin[20] proposed the so-called "global heating" model, based on a Taylor series of the surface resistance up to first order in temperature,

$$R_s = R_{s0}/(1 - CB_{\text{peak}}^2), \tag{6}$$

where R_{s0} and C are fitting parameters and $c = \gamma/b_C^2$.

The average correlation factor r^2 over fourteen fits for the three models and the three temperatures at which the RF tests were done are listed in Table IV. Table V contains the average values of the slope γ_{data} from model 1 at three different temperatures for all the baselines (before bake) and after all the baking.

It can be seen from Table V that the slope at 1.37 K before baking is about a factor of 2 higher than the slope at 2 K. The slopes also increase by about a factor of 2 with baking. A possible explanation for the medium field Q slope at $T < 2$ K is the presence of local losses and heating[21] that enhance the BCS surface resistance exponentially.

If we assume that the Taylor series of model 1 refers only to the BCS part of the surface resistance (T dependent) we can obtain an expression that relates the theoretical γ at 2 K given by Eq. (4) to measured quantities,

$$\gamma(2K) = [R_s(2\text{ K})\gamma_{\text{data}}(2\text{ K}) - R_{\text{res}}\gamma_{\text{data}}(1.37\text{ K})]/R_{\text{BCS}}(2\text{ K}). \tag{7}$$

The average value for the expression on the right-hand side is equal to 0.57 and is equal to the value given by Eq. (4) assuming a thermal conductivity of 6 W/(m K) and a Kapitza resistance of 1.25×10^{-4} $(\text{m}^2\text{K})/\text{W}$. Both these quantities are consistent with published values.[22]

TABLE III. Average values of the fitting parameters a and b of the low-field Q-slope model represented by Eq. (2).

	T=1.37 K		T=2 K	
	a [nΩ/(mT)^2]	b (nΩ)	a [nΩ/(mT)^2]	b (nΩ)
Before bake	24±8	4±1	28±9	21±2
After bake	40±13	6±1	34±14	15±2

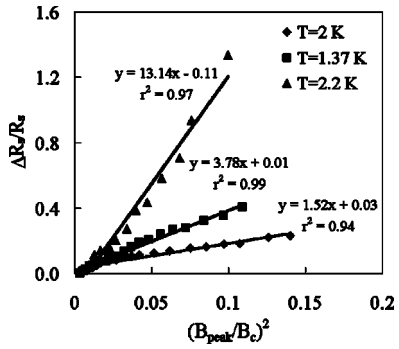

FIG. 21. Variation of surface resistance vs B^2_{peak} for the baseline data before 105 °C baking. Fitted functions according to model 1 are indicated.

On the other hand, the factor of 2 increase of the slope after baking would require that the Kapitza resistance be increased by a factor of 20. This could arise through oxidation of the outer surface of the cavity during bake-out but would require confirmation through direct measurement of Kapitza resistance after baking.

Above the superfluid transition temperature (2.17 K), the slope increases by about one order of magnitude. This is caused by heating of the RF inner surface of the cavity due to the poorer heat transfer capabilities of He I.

C. High-field *Q* drop

Field emission is the usual obstacle to achieving high accelerating gradients in superconducting cavities but sometimes the Q_0 versus field curve is characterized by a sharp decrease of the quality factor at high field in the absence of x-rays: the so-called "*Q* drop".

During these tests, this phenomenon was seen on two occasions and in both cases it disappeared after baking, as shown in Figs. 13 and 17. Such improvement has already been seen in many laboratories.[17,20]

We analyzed our data according to three models

(1) Halbritter explains the *Q* drop as due to interface tunnel exchange (ITE) between conduction electrons in niobium and localized states in the niobium pentoxide, causing losses due to the electric field.[23] This mechanism introduces an electric surface resistance that becomes important at high field (high enough to allow quasiparticles to cross the energy gap) and can be described by the following expression:

$$R_s^E = b[\exp(-c/E_p) - \exp(-c/E_0)], \tag{8}$$

where b, c, E_0 are fitting parameters.
E_0 represents the electric field onset for the *Q* drop. The electric surface resistance R_s^E can be obtained from the measured surface resistance from Eq. (3) as follows:

$$R_s^E = R_s/[1 + \gamma(B_{peak}/B_c)^2] - R_{s0}. \tag{9}$$

R_{s0} is the surface resistance at low field, where the electric component can be neglected.

(2) Saito proposed a model to explain the *Q* drop based on a temperature increase of the RF surface and a magnetic field dependence of the energy gap, according to the following formula:[24]

$$R_s = \frac{A}{T_0 + CB_{peak}} \exp\left[- \frac{B\sqrt{1 - \left(\frac{B_{peak}}{\sqrt{2}B_c}\right)^2}}{T_0 + CB_{peak}} \right] + R_{res}, \tag{10}$$

where A, B, and R_{res} are obtained from the fit of R_s vs $1/T$between 4.2 K and 1.37 K, while C and B_c are the fitting parameters.

(3) There is also a global heating model, described by Eq. (6).

Both models 2 and 3 are based on a magnetic field effect. The fits with model 2 do not give values of C and B_c that have physical meaning: C turns out to be negative and B_c is smaller than the values of B_{peak} actually measured. Models 3 and 1 can fit all our data very well. Figures 22 and 23 shows the results of the fit with models 3 and 1, respectively.

Table VI shows the values of the main fitting parameters for models 1 and 3 for the high-field *Q*-drop data. The values of E_0 obtained from the fits are within 1 MV/m of the measured peak electric field at which the *Q* drop starts.

Model 1 explains the shift of the *Q* drop to higher fields by baking as due to the reduction of the niobium pentoxide layer and therefore of the localized states and of the ITE

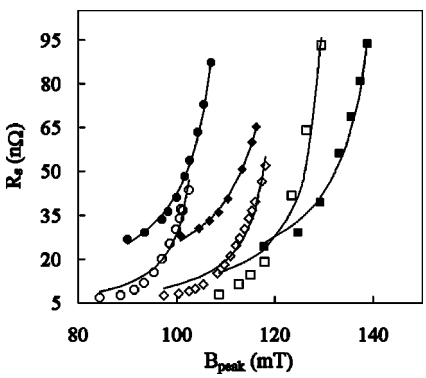

FIG. 22. R_s vs B_{peak}in the high-field *Q*-drop region from three different tests at 2 K (solid symbols) and 1.37 K (open symbols) fitted with model 3 (solid lines).

TABLE IV. Average correlation factors for the models describing the medium field *Q* slope at three different temperatures.

Model No.	Avg. r^2 (2.2 K)	Avg. r^2 (2 K)	Avg. r^2 (1.37 K)
1	0.966	0.822	0.974
2	0.868	0.955	0.957
3	0.717	0.606	0.849

TABLE V. Average values of the slope γ for all the tests obtained from the data fit with model 1.

	γ_{data} before bake	γ_{data} after bake
1.37 K	1.85±0.03	3.20±0.04
2 K	0.94±0.03	2.12±0.06
2.2 K	13.7±0.2	19.5±0.2

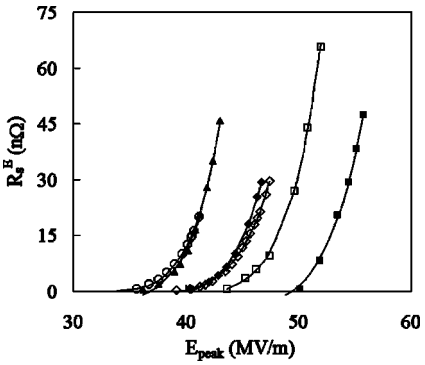

FIG. 23. Electric surface resistance from three different tests at 2 K (solid symbols) and 1.37 K (open symbols) fitted with model 1 (solid lines).

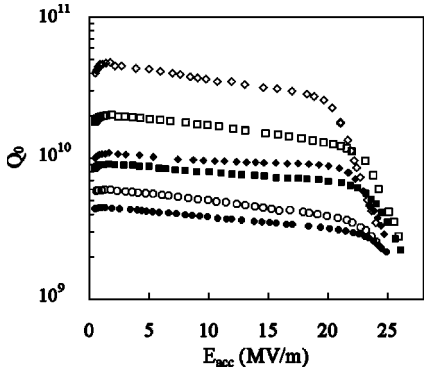

FIG. 24. Q_0 vs E_{acc} in the presence of 8 mG (diamonds), 32 mG (squares), and 140 mG (circles) residual dc magnetic field. Solid symbols refer to data taken at 2 K, open symbols refer to data taken at 1.37 K.

effect. The major problem with validation of this model is that results from temperature mapping of the cavity surface show heating in a broad area around the equator region where the magnetic field is stronger.[25]

The global heating model predicts a larger Q drop after baking, and is not consistent with the observed recovery of the effect after baking.

The possibility of the Q drop being caused by impurities (for example, tantalum) in the material is reduced by the high bulk RRR value of the cavity (>300) and by the fact that those impurities are uniformly distributed in niobium, while the RF field is only penetrating about 40 nm from the surface.

In the test before the 160 °C bake, the cavity was warmed to about 12 K and the residual dc magnetic field in the dewar was increased. This operation was repeated a few times to look for any influence on the Q drop. As can be seen in Fig. 24, although the residual resistance is increasing due to the dc magnetic field being trapped during the cool-down,[26] there is no significant variation in the behavior of the Q drop.

V. CONCLUSION

Baking a niobium cavity for 48 h at temperatures greater than 100 °C causes the following effects.

(1) Reduction of the BCS surface resistance at 4.2 K by as much as 50% and improvement of the cavity quality factor at 2 K by as much as 20%.
(2) Modification of the oxide structure and oxygen diffusion in the niobium, causing a reduction in the mean free path.
(3) Release of hydrogen from the surface as shown by the NRA measurements.
(4) An increase of Q_0 with increasing field in the low-field regime, in a manner consistent with the model proposed by Halbritter of NbO_x clusters not in thermal equilibrium with the surrounding niobium.
(5) An apparent substantial increase in the Kapitza resistance that must be confirmed by additional direct measurements.
(6) An increase in the medium field Q slope, possibly through local losses.
(7) Elimination of the high-field Q drop after baking at 120 °C and 160 °C. These data are well described by the ITE model, related to electric field, and by global heating model, related to magnetic field. On the other hand, both models are in conflict with some experimental observations.[27] After baking at 120, 160, and 180 °C, the cavity is limited by thermal quench, which was not reached before bake out. Also, the quench field decreases as the baking temperature is increased. This is consistent with the reduction of thermodynamic critical field observed in a cavity baked at 150 °C for 48 h (Ref. 28) in oxygen.
(8) A residual dc magnetic field does not seem to influence the behavior of the Q drop.

ACKNOWLEDGMENTS

We would like to thank P. Kneisel for his help and support throughout this experimental program, W. L. Lanford for the NRA measurements, and J. Halbritter for many useful discussions and a review of this paper. We would also like to

TABLE VI. Main fitting parameters and correlation factors for the surface resistance fit of the Q drop with models 1 and 3.

	Model 1				Model 3	
Test No.	$b(\Omega)$	c(MV/m)	E_0(MV/m)	r^2	$C[1/(\mathrm{mT})^2]$	r^2
9 at 2 K	1.34	820	40.5	0.999	$6.36E-5$	0.996
9 at 1.37 K	0.52	789	39.5	0.999	$6.69E-5$	0.966
11 at 2 K	0.57	700	36.9	0.997	$7.81E-5$	0.994
11 at 1.37 K	0.30	679	34.7	0.999	$8.84E-5$	0.958

thank J. Delayen and G. Rao for helpful discussions. This work was supported by the U.S. DOE Contract No. DE-AC05-84ER40150.

[1]S. Calatroni, C. Benvenuti, and V. Ruzinov, 10th Workshop on RF Superconductivity, Tsukuba, Japan, 2001.
[2]Q. Ma and R. A. Rosenberg, 10th Workshop on RF Superconductivity, Tsukuba, Japan, 2001.
[3]B. Bonin and R. W. Roeth, 5th Workshop on RF Superconductivity, Hamburg, Germany, 1991.
[4]W. A. Lanford, Nucl. Instrum. Methods Phys. Res. B **66**, 65 (1992).
[5]URL: http://www.jlab.org
[6]J. Halbritter, J. Appl. Phys. **41**, 4581 (1971).
[7]G. Ciovati, JLAB-TN-03-003, 2003.
[8]J. Halbritter, FZK 3/70-6, 1970.
[9]P. Kneisel, O. Stoltz, and J. Halbritter, J. Appl. Phys. **45**, 2296 (1974).
[10]A. Phillipp and J. Halbritter, IEEE Trans. Magn. **19**, 999 (1983).
[11]J. Halbritter, Z. Phys. **266**, 209 (1974).
[12]R. Schwab, Externer Bericht 6023, FZK Karlsruhe, 1997.
[13]C. C. Koch, J. O. Scarbrough, and D. M. Kroeger, Phys. Rev. B **9**, 888 (1974).
[14]A. Dacca′, G. Gemme, L. Mattera, and R. Parodi, Appl. Surf. Sci. **126**, 219 (1998).
[15]C. Z. Antoine, A. Aspart, M. Berthelot, Y. Gasser, J. P. Poupeau, and F. Valin, 9th Workshop on RF Superconductivity, Albuquerque, NM.
[16]K. Kowalski, A. Bernasik, W. Singer, W. Singer, and J. Camra, 11th Workshop on RF Superconductivity, Travemuende, Germany, 2003.
[17]P. Kneisel, 9th Workshop on RF Superconductivity, Albuquerque, NM, 1999.
[18]J. Halbritter, 1st Workshop on RF Superconductivity, Karlsruhe, Germany, 1980.
[19]J. Halbritter, 38th Eloisatron Workshop, Erice, Italy, 1999.
[20]B. Visentin, J. P. Charrier, B. Coadou, and D. Roudier, 9th Workshop on RF Superconductivity, Albuquerque, 1999.
[21]J. Halbritter, 11th Workshop on RF Superconductivity, Travemuende, Germany, 2003.
[22]M. Fouaidy, S. Bousson, T. Junquera, N. Hammoudi, J. C. Le Scornet, and J. Lesrel, 9th Workshop on RF Superconductivity, Albuquerque, NM, 1999.
[23]J. Halbritter, IEEE Trans. Appl. Supercond. **11**, 1864 (2001).
[24]K. Saito, 2003 Particle Accelerator Conference, Portland, OR, 2003.
[25]G. Eremeev, M. Liepe, H. Padamsee, and R. Roy, 11th Workshop on RF Superconductivity, Travemuende, Germany, 2003.
[26]M. Ono, E. Kako, T. Shishido, S. Noguchi, and T. Yokoi, 9th Workshop on RF Superconductivity, Albuquerque, 1999.
[27]B. Visentin, 11th Workshop on RF Superconductivity, Travemuende, Germany, 2003.
[28]J. Knobloch, R. L. Geng, M. Liepe, and H. Padamsee, 9th Workshop on RF Superconductivity, Albuquerque, NM, 1999.